

LA-UR-82-601-1

Page 1 of 1

TITLE GENERATION OF VACUUM ULTRAVIOLET RADIATION BY PLASMA NONLINEARITIES

AUTHOR(S) R. L. Carman, X-1
C. H. Aldrich, X-1

MASTER

SUBMITTED TO Topical Meeting on Laser Techniques for Extreme Ultraviolet
Spectroscopy Optical Society of America,
Boulder, Colorado, March 8-10, 1982

 By acceptance of this article, the publisher acknowledges that the U.S. Government retains a non-exclusive, royalty-free license to publish or reproduce it, or parts of it, in any medium, without prior permission or payment to the author(s).

The Los Alamos National Laboratory requests that the publisher identify this article as work performed under the auspices of the U.S. Department of Energy.

Los Alamos Los Alamos National Laboratory
Los Alamos, New Mexico 87545

Generation of Vacuum Ultraviolet Radiation
by Plasma Nonlinearities*

R. L. Carman and C. Aldrich

University of California
Los Alamos National Laboratory
Los Alamos, NM 87545

ABSTRACT

Numerical simulations of the relevant plasma hydrodynamics indicate that ten (19.3 μm) or more harmonics of an ArF laser should be generated at high efficiency in a high irradiance solid target plasma interaction experiment.

*Work performed under the auspices of the U. S. Department of Energy.

Introduction

The observation of very high harmonic light in CO_2 laser plasma interaction experiments¹ and the subsequent experimental study of the properties of this radiation^{2,3} have led to a revived interest in the theory of harmonic generation in laser produced plasmas. We will begin with a brief review of the key experimental results and the current theoretical situation for CO_2 laser plasmas. We then turn our attention to a theoretical extension of this work to shorter wavelength irradiation systems where we shall predict that optical harmonics should be produced in the vacuum ultraviolet. When we use the ArF laser for a high irradiance source, up to five harmonics are predicted for pulse widths of < 10 ps, and even more harmonics may be possible for pulse widths of < 2 ps. Several uncertainties in the calculations make it difficult to be very precise, but the results are sufficiently interesting to suggest that the ideas be pursued experimentally.

High Irradiance CO_2 Laser-Plasma Interaction Results

In early work, we noted that for CO_2 laser intensities of $I_L > 10^{14} \text{ W/cm}^2$, the behavior of the harmonic conversion efficiency with harmonic order changed from an approximate linear fall-off with order⁴, to one which was almost constant in conversion efficiency to greater than 20 harmonics, with a subsequent rapid fall-off.¹ The number of harmonics appeared to be approximately independent of the solid target material while the angular distribution appeared to be approximately flat, leading to conversion efficiency estimates of 10^{-4} to 10^{-5} of the

incident energy converted to each harmonic order. Repeating the Gemini laser facility experiments at the Helios laser facility, with incident intensities of up to $I_L \sim 3 \times 10^{16} \text{ W/cm}^2$, indicated that more than 3 harmonics were efficiently produced with higher conversion efficiency, constant to within 50% of each other, thus suggesting a correlation between the maximum harmonic efficiently produced n and incident laser intensity I_L .

Two dimension particle simulations were carried out¹ under conditions where collisions could be ignored but where Maxwell's equations were solved exactly. For incident laser intensities of I_L 10^{14} W/cm^2 to 10^{15} W/cm^2 , we observed a correlation between the number of harmonics predicted and the features of the plasma density profile modification. The Fourier transform of the scattered or reflected light power showed the constant harmonic conversion efficiency over several harmonic orders. Also, the upper shelf density of the profile modification, caused by the radiation pressure balancing the hydrodynamic expansion pressure, was found to nearly coincide with the critical density for the highest harmonic efficiently produced. The lower-shelf density of the profile modification was found to be approximately one-tenth the critical density for the CO₂ light, while the density jump from 10^{19} e/cc to $\sim 7 \times 10^{20} \text{ e/cc}$ occurred over ~ 1 um in space when 8 harmonics were efficiently produced. The conclusion drawn was that an approximate phase matching was taking place. When the skin depths for each of the harmonics and the incident CO₂ radiation approximately coincided, the harmonic conversion efficiency was high.

However, for harmonics whose corresponding critical density was above the upper-shelf density, this phase matching was no longer satisfied and the conversion efficiency was therefore substantially reduced.

The origin of the plasma nonlinearity was also indicated by the calculations.¹ The plasma profile modification was known to be driven by the resonant absorption process. Here the light polarized in the plane of incidence couples to a surface Langmuir plasma wave. The high laser intensity causes steepening of this plasma wave, and its subsequent radiation is the harmonic light, but this same steepening was also found to be closely associated with the ejection of hot electrons. Thus, the light wave was impulsively accelerating the electrons, causing some to be ejected, and the collective plasma response was to cause highly non sinusoidal Langmuir waves to be excited, from which the harmonic light originates.

This formed a neat package, but was largely still quite speculative. Also, some disagreements with predictions already existed. For example, the theory required the laser irradiation to be polarized in the plane of incidence while all the experiments were carried out with the irradiation polarized normal to the plane incidence. Furthermore, the theory suggested that the harmonic light should be radiated in the specular reflection direction and not into all angles in the backward half space. However, the simulations were carried out for a plane wave which does not produce cratering in the plasma while ripples in the critical surface could also cause similar effects.

We attempted to check the theory quantitatively in a dedicated series of experiments at the Gemini laser facility² using $I_L < 10^{15} \text{ W/cm}^2$. Also, one or two more results were obtained at the Helios laser facility.^{2,3} We found that quantitative checks of the number of harmonics efficiently generated and the upper shelf density consistent with the radiation-driven density-profile modification could only agree if the cold-plasma temperature T_c were between 10 and 120 eV. This can be seen from the relationship²

$$P_{\text{radiation}} = \frac{E^2}{8\pi} (2-A) = P_{\text{hydro}} = N_{\text{upper}} T_c. \quad (1)$$

Where P is the pressure, A is the absorption fraction and N_{upper} is essentially the critical density for the last efficiently generated harmonic n , implying $N_{\text{upper}} = n^2 N_{\text{crit}}$. Here $N_{\text{crit}} = 10^{19} \text{ e/cc}$ is the critical density for the incident CO_2 radiation. Streak camera studies of the harmonic light revealed that the visible harmonic pulse width was typically $\sim 200 \text{ ps}$, while absolute timing checks indicated that the harmonic light was emitted only during the rise of the CO_2 laser pulse, which was 200 ps . The remaining $\sim 800 \text{ ps}$ to 1.2 ns falltime of the CO_2 pulse produced no visible harmonics. In contrast, work at Helios, and elsewhere,⁶ found that the infrared harmonic light was generated throughout the whole laser pulse. While greater than 50 harmonics were sometimes observed to be efficiently generated, the laser intensity required was actually less than the maximum available, while at maximum irradiance we had one example of no visible harmonics being produced. High resolution spectra

were then taken, an example of which is shown in Fig. 1. This spectrum is of the 16th harmonic of the P(20) transition in the 10.6 μm band, and was obtained at Helios, where the output is principally on the P(20) transition, although P(16), P(18), and P(22) are also present in the output. The frequency bandwidth of all the observed visible harmonics is $\sim 100 \text{ cm}^{-1}$ and is the same whether only the P(20) rotational-vibrational line is lasing or if four transitions are lasing. The spectrum, of Fig. 1, appears to have both a fine and a more coarse periodicity. Careful analysis reveals a $1.8 \pm 0.05 \text{ cm}^{-1}$ uniform periodicity across the entire spectrum, while portions of the spectrum display an $\sim 9 \text{ cm}^{-1}$ lower frequency modulation. The spectrum is centered to $\sim 1 \text{ cm}^{-1}$ at the 16th harmonic of P(20). While the 1.8 cm^{-1} periodicity can be explained as a beating of the 4 transitions whose average spacing is 1.79 cm^{-1} , nearly 100 orders are visible in the spectrum suggesting that the associated four-wave mixing phenomena had to be iterated several times.³ The lower modulation frequency of 9 cm^{-1} is believed to be associated with self-phase modulation. If this interpretation is correct, the existence of both of these effects provides indirect evidence for self focusing in the underdense plasma. X-ray pin hole camera data² further suggested that self focusing may be occurring, since higher incidence intensity corresponded to more broken-up $\sim 1 \text{ keV}$ x-ray emission patterns.² If self focusing was occurring, it would imply higher intensities could exist locally in the focal region and, therefore, permit T_c to be substantially higher, as inferred from Eq. (1). Since T_c is thought to be nearly 1 keV, an intensity increase of between 10 and 100-fold would thus be inferred. The existence of the high harmonic light only on the rise of the CO₂ pulse then implied that the self focussing only occurred during this time.

In an attempt to rule out other possible explanations to self focussing, we decided to try a second dedicated series of experiments in which the laser risetime was varied while the visible harmonic production was monitored. Here we found, for CO₂ laser pulse risetime much greater than 200 ps, no visible harmonics were efficiently produced even for peak intensities $I_L \sim 2 \times 10^{15} \text{ W/cm}^2$. Similarly, the presence of a prepulse also precluded even the 13th harmonic from being efficiently produced. Since the presence of large quantities of underdense plasma should have improved the probability of self focussing, these results suggested that while self-focussing may be occurring, n did not depend on the incombant light intensification. In contrast, for CO₂ laser risetimes of ~ 100 ps (the shortest available) we found that the largest number of harmonics were efficiently produced. In fact, $n = 50$ for $I_L = 2.3 \times 10^{15} \text{ W/cm}^2$ and $\tau_{\text{rise}} = 125$ ps, while $n = 42$ for $I_L = 4.9 \times 10^{15} \text{ W/cm}^2$, and $\tau_{\text{rise}} = 160$ ps clearly indicates the overall importance of the laser risetime.

Transient Hydrodynamic Theory of High Harmonic Production for CO₂ Laser

Plasma Experiments

Despite the ability of particle simulations to probe the plasma instabilities and nonlinear coupling associated with this problem, the approach had to be abandoned for several reasons. PIC calculations are usually utilized for collisionless plasmas, while applying the relation $N_{\text{upper}} = n^2 N_{\text{crit}}$ to problems where $n = 50$ indicates that $N_{\text{upper}} \sim 2-3 \times 10^{22} \text{ c/cc}$. For these densities, collisional effects are clearly very important. Also, with Cray computers, PIC calculations are practical only for time scales of a few hundred optical cycles, or for 10-20 ps, when a range of about 10^3 to 10^4 in plasma density is

requested. But what is required is that all densities from $N < 0.1$ $N_{\text{crit}} \sim 10^{18}$ e/cc to fully ionized solid densities, where $N > 10^{24}$ e/cc be present for simulation times of 100–200 ps. The presence of large shocks may dictate an even more extreme range of conditions be modeled.

An alternative to the PIC simulation was to use a hydrodynamics code to predict the density profiles and then solve the electromagnetic problem separately. Since the origin of many of the phenomenological models contained in Lasnex (a hydro code) were PIC simulations, Lasnex seemed to be a logical starting point. In particular, the hot-electron production model, the radiation pressure model and the resonant absorption model in Lasnex came from PIC simulations. However, to accurately describe the relevant range in density requires very fine zoning and long computation times. Also, this use of Lasnex has aggravated a few problems which exist in the code, while causing us to discover a few new problems.

The physics we will be applying is essentially that discussed above, except that N_{upper} is no longer given by radiation-pressure balance. Instead N_{upper} is a dynamic quantity which is given by the density to which the CO_2 laser radiation can penetrate, namely the maximum plasma density which is spatially within one optical skin depth, for the irradiating laser, of its critical density. We first apply this approach to a lower intensity CO_2 irradiation where PIC simulations exist and good data exist. Figure 2 shows the Lasnex¹ results for a 200 μm radius glass microballoon (GMB) overcoated with 15 μm of plastic. The assumed laser pulse shape is shown in Fig. 3 (top). However, for Lasnex the hot-electron generation has been turned off, which leads to essentially exponential density profiles;

$$N_e \sim [a \ln(t/t_0) - b] e^{z/z_0}, \quad (2)$$

where $a = 9.68 \times 10^{20}$ e/cc, $b = 1.54 \times 10^{21}$ e/cc, $c = 1.6 \mu\text{m}$, $d = 2.067$, $t_0 = 1 \text{ ps}$, and $z_0 = c t^d$. Now, using our exact numerical solution of Maxwell's equations in the presence of a steep density gradient, we can find the skin depth and hence N_{upper} . For an exponential falloff of plasma density with distance z , we find a good analytic fit to the skin depth δ , for 10 μm radiation, namely

$$\delta = 1.24 z_0^{0.538}. \quad (3)$$

Combining these results, we then arrive at Fig. 3 (bottom), which plots both I_L and the derived N_{upper} as a function of time. Now, the harmonic light will be efficiently produced over the time scale where N_{upper} is overdense to that harmonic. Because of the high power-law dependence of the visible harmonic light on intensity, we should expect some variation in the generation efficiency with incident laser intensity. No such strong dependence is inferred from the data suggesting that the harmonic generation efficiency is saturated in some sense. We, therefore, do not take this into account. From Fig. 3 (bottom), we would predict a monotonic fall-off of harmonic conversion with n .

Repeating the Lasnex¹ calculation, but with the hot electron generator turned on, yields the Lasnex 2 results of Fig. 2. Note the qualitative changes in the hydrodynamics. In particular, the expansion is slowed markedly because the cold-plasma temperature has been reduced. Also, the radiation-pressure effects are now sufficient, even early in the irradiation causing some steepening of the density profile.

Both the Lasnex 1 and Lasnex 2 calculations were done for $I_{\max} = 1.5 \times 10^{13} \text{ W/cm}^2$ or $I\lambda^2 = 1.7 \times 10^{15} (\mu\text{m})^2 \text{ W/cm}^2$. In order to understand the effects of increasing the incident CO_2 laser intensity, the Lasnex 4 calculation was performed. Here the laser intensity is now $I_{\max} = 2 \times 10^{14} \text{ W/cm}^2$. Both the increase in hot-electron temperature and in radiation pressure has caused the density profile to steepen even more than that of Lasnex 2, where

$$T_{\text{hot}} \approx 56[I\lambda^2 T_c]^{1/3} \text{ (keV).} \quad (4)$$

The units are $\lambda(\mu\text{m})$, $I(10^{16} \text{ W/cm}^2)$, and T_c (keV). This T_{hot} is approximately 4 times the previously published Los Alamos result,⁷ and is a better fit to present data for $10^{14} < I_L < 10^{16} \text{ W/cm}^2$. To construct the plot of N_{upper} versus time for Lasnex 4, a cubic spline fit to the density profiles is fed into the electromagnetic code to first fine the skin depth and then N_{upper} . The results suggest that the third and fourth harmonic should be produced at about the same efficiency, while the fifth and higher should be produced with a monotonically decreasing efficiency, consistent with both early particle simulations¹ and the experimental data in Refs. 4 and 5.

Lasnex calculations for $I_L \sim 3 \times 10^{16} \text{ W/cm}^2$ have also been performed, but severe difficulties developed due to the $T_{\text{hot}} \sim 400 \text{ keV}$ near N_{crit} . Basically, the hot-electron transport and the coupling of the hot electrons to both the ion distribution and the cold electron distribution in the underdense plasma are not sufficiently well described to provide for a detailed description of the density profiles. Work is underway to try to remedy these problems.

Application of the Transient Hydrodynamic Theory to High Irradiance ArF
Laser-Plasma Experiments

A significant difference in the techniques for modeling CO₂ laser-plasma experiments and present uv laser-plasma experiments must be taken into account in order to use Lasnex for these uv calculations. The uv absorption experimentally is principally by the inverse-bremsstrahlung process which does not lead to hot-electron production. However, the thermal electron flux must be limited to about 3% of that expected by the Spitzer conductivity. For incident intensities $I_L < 10^{15} \text{ W/cm}^2$, the radiation pressure effects for ultraviolet laser will also be neglectable. Another experimental result is that the hot-electron temperature associated with 0.35 μm laser-plasma experiments has a weak dependence on the atomic number Z of the target, namely $\bar{Z}^{1/4}$, where \bar{Z} is the state of ionization of the material; for example, for helium-like copper, $\bar{Z} = 27$. Thus, the higher T_c coupled with the absence of profile modification effects suggest that we should expect the hydrodynamics to proceed similar to that of the Lasnex 1 calculations of Fig. 2.

Guided by the Lasnex 2 and Lasnex 4 results above, we suspect that high-harmonic generation by an ArF laser will become efficient only if hydrodynamic expansion can be greatly diminished. Short pulses with very fast risetimes will satisfy this requirement. For $I_L > 10^{16} \text{ W/cm}^2$, $I_L^2 > 3 \times 10^{14} (\mu\text{m})^2 \text{ W/cm}^2$ and we now expect radiation-pressure effects to be important. Furthermore, when we combine the two above, inverse bremsstrahlung absorption will no longer be as important, since

the density gradient scale height will be insufficient. Thus, in analogy to the high irradiance 1.06 μm and 10.6 μm laser plasma results, we will expect resonant absorption to become more important, implying the excitation of surface Longmuir plasma waves, the production of hot electrons, and the potential for producing harmonic light.

The Lasnex 3 calculation of Fig. 4 gives the density profiles associated with an ArF target irradiation at $I_L = 2 \times 10^{15} \text{ W/cm}^2$. The target is a 15 μm copper overcoated 200 μm radius GME. $T_{\text{hot}} = 56 \text{ keV}$ is obtained from Eq. (4), where $T_c = 11 \text{ keV}$ and we have also multiplied by $(\bar{Z})^{1/4}$ with $\bar{Z} = 27$. While this T_{hot} is higher than would be inferred from present target experiments using 0.35 and 0.26 μm lasers, they are carried out under conditions which are substantially different than those described above. The assumed irradiation conditions here more closely approximate those associated with CO₂ laser-plasma experiments at Los Alamos. As a further justification for using this T_{hot} , we note that several plasma instabilities could be driven at such high intensities, while many of these instabilities produce hot electrons.

When the results of Lasnex 3 are processed as described above, we predict a substantial conversion to the first seven ArF harmonics, namely 193 nm, 96.5 nm, 64.3 nm, 48.3 nm, 38.6 nm, 32.2 nm, and 27.6 nm. The total absorption expected by the calculation is ____ of which ____ is by resonant absorption. Note that the solid electron density in an uncompressed condition corresponds to $N_e \sim 3 \times 10^{23} \text{ e/cc}$, so that the surface material has been shocked up to approximately 4 times solid density. From this result we thus see how to further increase the number

of potential harmonics, namely to further shock the surface material. In principal, it is possible to shock the material up to ~ 25 times normal density or $N_e \sim 7.5 \times 10^{24}$ e/cc, which could lead to $n = 16$. We have not been able to achieve this result using Lasnex. Rather, the highest electron density we have been able to achieve at the surface is $N_e < 3 \times 10^{24}$ e/cc, and this required an $I_L \sim 5 \times 10^{16}$ W/cm² focused on a molybdenum target. Since we are again approaching plasma conditions where Lasnex is less likely to predict correctly the hydrodynamics, we regard this result as even more speculative. At this point, we wish to stress that the lack of adequate laser produced plasma data and models applicable to this wavelength, intensity, and pulse width regime have forced assumptions to be made which may not be justified. On the other hand, no assumptions have been made which are inconsistent with our present understanding.

In conclusion, we believe that short pulse, high irradiance laser-plasma experiments utilizing an ArF laser have the potential for producing several vacuum ultraviolet wavelengths down to possibly 19.3 nm. Through these sources should be diverging possibly hemispherically, the use of lenses (Fresnel zone plates) should allow a fair portion of the harmonic light to be recollimated if so desired, while the use of this harmonic light as a flashlamp, a holographic source, or a probe might be potentially interesting.

The authors wish to thank Eldon Linnebur, David Forslund, Jerry Blackbill, John Lindl, Keith Boyer and Charles Rhodes for very helpful discussions during the progress of this work.

References

1. R. L. Carman, D. W. Forslund, and J. M. Kindel, *Phys. Rev. Lett.* 46, 29 (1981).
2. R. L. Carman, C. K. Rhodes, and R. F. Benjamin, *Phys. Rev. A* 24, 2649 (1981).
3. R. L. Carman, "Factors Affecting Target Irradiation Symmetry in CO₂ Laser Fusion Experiments," *Proc. Topical Conf. on Symmetry Aspects of Inertial Fusion Implosions* (to be published); also Los Alamos National Laboratory Report LA-UR-81-1566 (1981).
4. N. H. Burnett, H. A. Baldes, M. C. Richardson, and G. D. Enright, *Appl. Phys. Lett.* 31, 172 (1977) and references therein.
5. E. A. McLean, J. A. Stamper, B. H. Ripin, H. R. Griem, J. McMahon, and S. E. Bodner, *Appl. Phys. Lett.* 31, 825 (1977) and references therein.
6. P. A. Jaanimagi, G. D. Enright, and M. C. Richardson, *IEEE Trans. Plasma Sci.* P57, 166 (1979).
7. See, for example, D. W. Forslund, J. M. Kindel, and K. Lee, *Phys. Rev. Lett.* 39, 284 (1977) and references therein.

Figure Captions

Fig. 1. High resolution spectrum of 16th harmonic generated in a CO₂ laser plasma experiment. Note the high degree of frequency modulation.

Fig. 2. Two Lasnex hydro calculations with (1) and without (2) the presence of hot electrons. Note the qualitative change in the resulting density profiles.

Fig. 3. Plot of the assumed laser pulse shapes for all Lasnex calculations (top). Plot of the rising portion of I_L and the inferred variation in N_{upper} for the Lasnex 1 hydrodynamics, as defined in the text.

Fig. 4. Two Lasnex hydro calculations (3) ArF laser of 0.875 ps rise, 9 ps FWHM, and 2 ps peak intensity and (4) CO₂ laser of 87.5 ps rise, 900 ps FWHM, and 200 ps peak intensity. Note the high hot-electron temperatures (see text.).

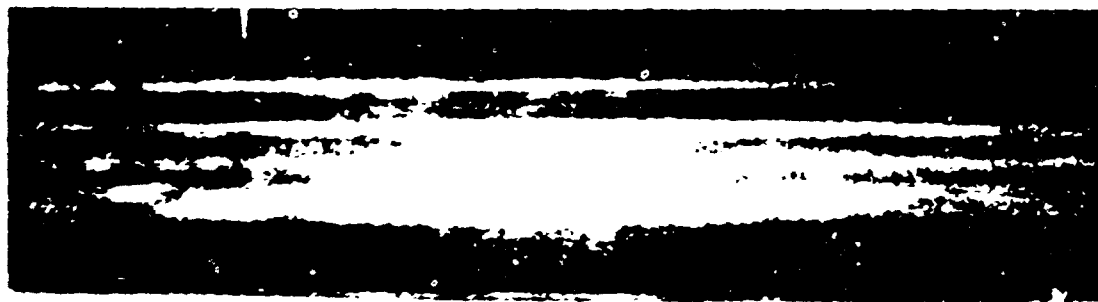
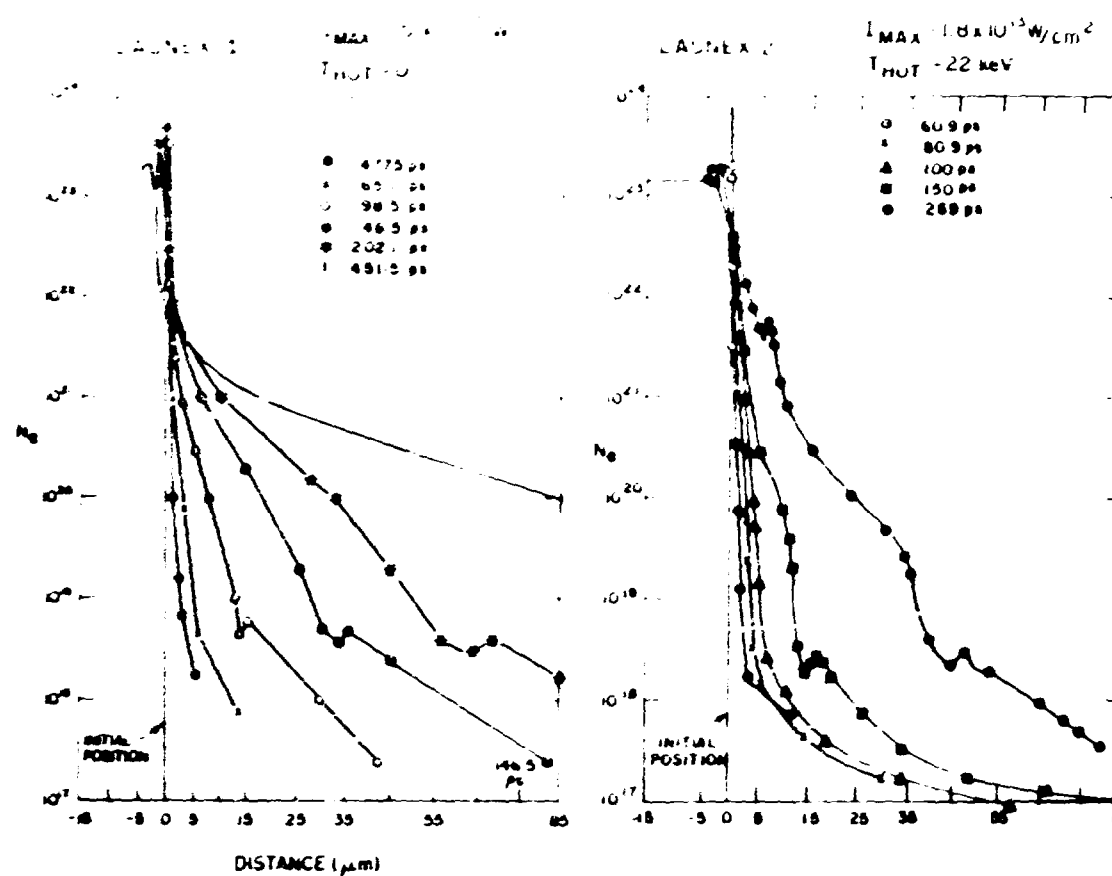


Fig. 2. A photograph of the surface of a 100-
μm thick film of polyethylene irradiated
with a dose of 100 Mrads at 22 keV
and then annealed at 100°C for 1 hr.



The dose rate distribution will be affected by annealing.

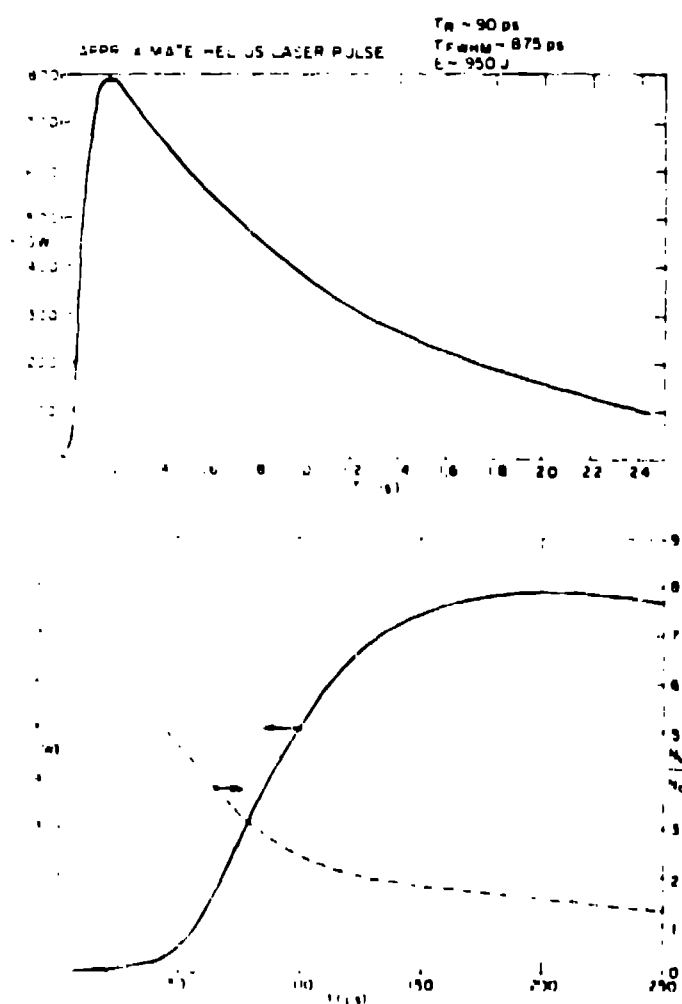


Fig. 3. ~~Calculated~~
 Plot of the relative energy
 pulse width to ~~the~~
 of the calculation
 (Fig. 1) of the
 of the laser pulse
 and the reflected pulse
 in hydrogen experiment
 in the

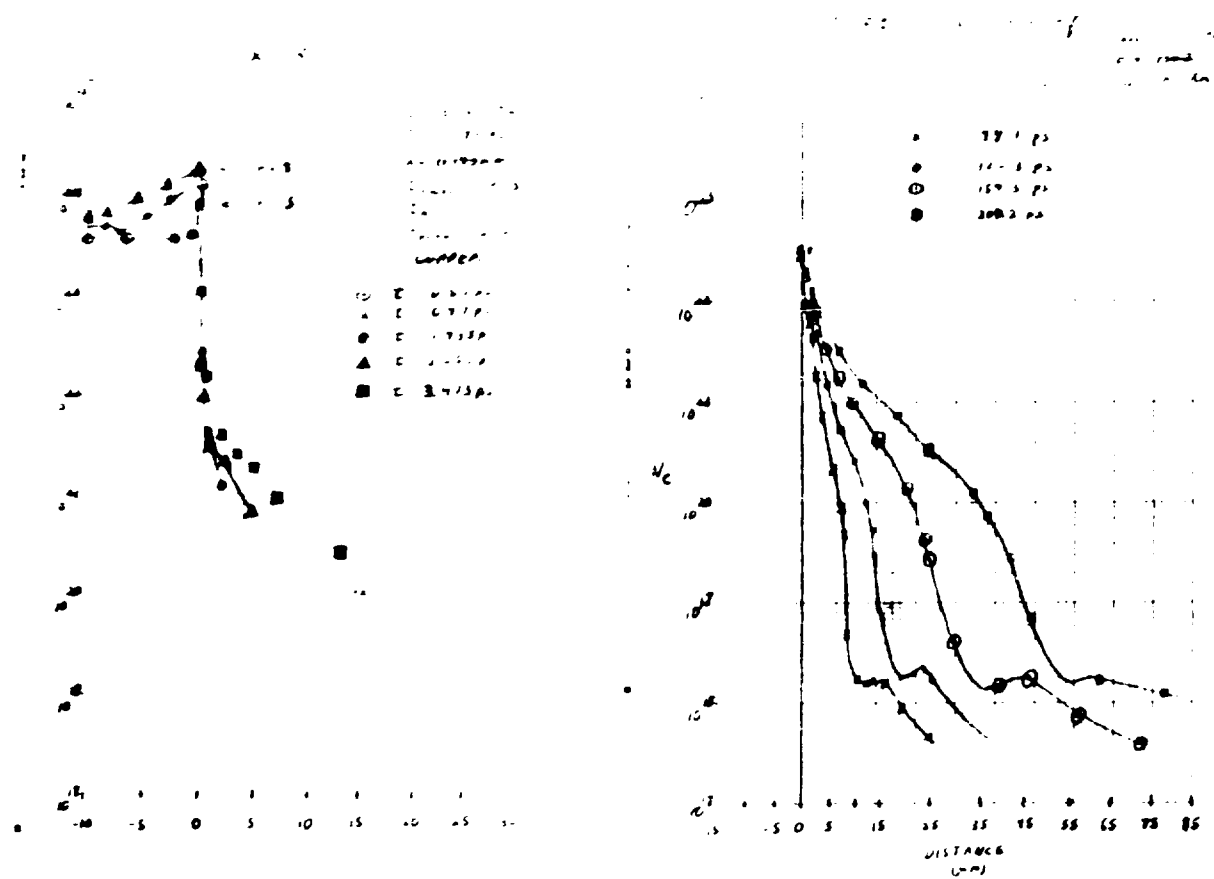


Fig. 4. The same hydrodynamic conditions (3) from Artiller
experiments reactions (p) and (1) from the case of
825 p reactions, and (2) (3).